# DOWNSCALING CLIMATE PROJECTIONS IN TOPOGRAPHICALLY DIVERSE LANDSCAPES OF THE COLORADO PLATEAU IN THE ARID SOUTHWESTERN UNITED STATES

*Gregg M. Garfin, Jon K. Eischeid, Melanie Lenart, Kenneth L. Cole, Kirsten Ironside, and Neil Cobb*

## ABSTRACT

Global Climate Models (GCMs) operate at scales much larger than the federal and state forest, range and riparian ecosystems managed by land and water professionals. Therefore, incorporating information on climate change projections into resource management plans requires GCM projections at a scale more relevant to ecosystems, especially in topographically diverse regions such as the western United States. In an effort to address this need, we developed downscaled climate projections for the Southern Colorado Plateau (SCP) (35° to 38°N, 114° to 107°W), centered on the Four Corners states. We compared twenty-two global climate models (GCMs) from the archive of model runs used in the Intergovernmental Panel on Climate Change Fourth Assessment Report, and statistically downscaled them to a 4 km grid, to accord with spatially and temporally continuous historic observations using the Parameter-elevation Regressions on Independent Slopes Model (PRISM) data set. From these results, we selected five models representing a range of plausible possible climate futures. We consider them in the context of three seasonal time frames observed to be critical for vegetation in the SCP: winter (November–March), arid foresummer (May–June), and summer monsoon (July–September). Projections for the SCP describe a warmer future, in which annual temperatures seem likely to increase by 1.5° to 3.6°C by mid-century, and 2.5° to 5.4°C by the end of the century, depending on the model chosen. Annual temperatures are projected to exceed the 1950–1999 range of variability by the 2030s. Annual precipitation changes are more equivocal. A conservative estimate, using a 22-model ensemble average, indicates that SCP annual precipitation may decrease by 6% by the end of the century. For precipitation projections, GCM agreement is greatest for the May–June arid foresummer season, and projections show SCP May–June precipitation declining by 11 to 45% during the twenty-first century. Downscaled output from this study will be used to drive vegetation change models with the intent of examining a diversity of possible outcomes so scientists can test an array of vegetation changes, and resource managers can make informed decisions in relation to the range of possible climate change scenarios.

## INTRODUCTION

This paper describes the process and results of Global Climate Model (GCM) selection and statistical downscaling of climate parameters for use by ecologists examining vegetation change in the Southern Colorado Plateau (Figure 1). The downscaled climate data will eventually be used as input into

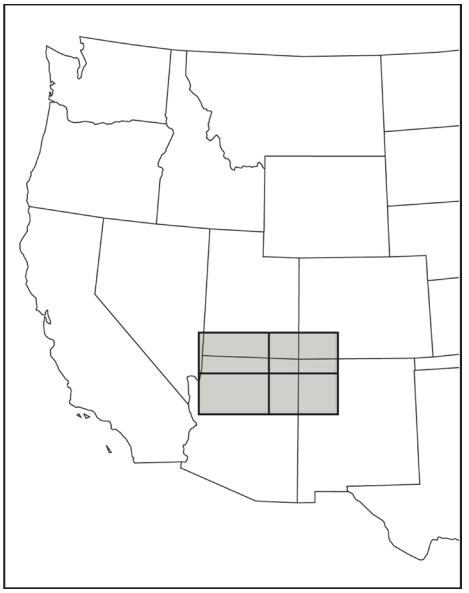

**Figure 1.** Western United States and Southern Colorado Plateau (shaded box) domains used in this study.

process-based, landscape-scale vegetation models. The impetus for the study is scientific and public interest regarding the recent rapid and massive forest mortality on the Southern Colorado Plateau (SCP), which affected nearly 1.4 million hectares of forest land between 2002 and 2004 (USDA 2008). Given coarse spatial scale projections of a warmer drier Southwest (Seager et al. 2007), there is concern that such changes may presage future ecosystem changes in the region. Research on pinyon pine mortality in the SCP suggests that a combination of drought and unusually high temperatures depleted soil moisture to a greater extent during a recent drought episode than during past drought episodes, thus exposing trees to "global-change-style" drought stress (Adams et al. 2009, Breshears et al. 2005). Moreover, researchers speculate that increasing temperatures also enhance insect life cycles and predispose Southwestern forests to greater risk of massive mortality in response to drought (Stephenson et al. 2006, Burkett et al. 2005, Logan et al. 2003).

Global Climate Model (GCM) grid cells, the areal unit at which parameters are projected by the models, are often larger than 1 degree latitude and longitude per side (~100 km in mid-latitudes). In a region as topographically diverse as the Colorado Plateau, having a single value for a parameter such as precipitation makes it challenging for resource managers to consider how temperature and precipitation changes will impact the considerably smaller than GCM grid cell-sized forest, range, and riparian ecosystems that they manage. For example, the dramatic topography of the San Francisco Peaks of northern Arizona would take up only a small fraction of a 1°x1° grid cell, and their effect on local climate and hydrology would be greatly attenuated. Although statistically downscaling GCM projections to finer spatial scales cannot remove so-called epistemic uncertainties (e.g., imperfect knowledge of some climate system processes), improving the spatial scale of GCM estimates to the point where the effects of regional elevation can be approximated should help improve estimates. The addition of such detail in model projections could provide guidance needed by land managers to discern projected temperature differences between mountain ranges and adjacent rangelands, and to better evaluate management strategies and climate change adaptation options (e.g., Bachelet et al. 2003). While modelers work to improve spatial resolution and dynamical processes within the next generation of models, relatively quick and cost-effective statistical downscaling efforts can allow scientists and managers to evaluate more finely detailed and plausible potential impacts based on the array of current generation GCM projections.

Climate has long been known to be important in determining the distribution of native plants on the landscape. The physiological adaptations of individual

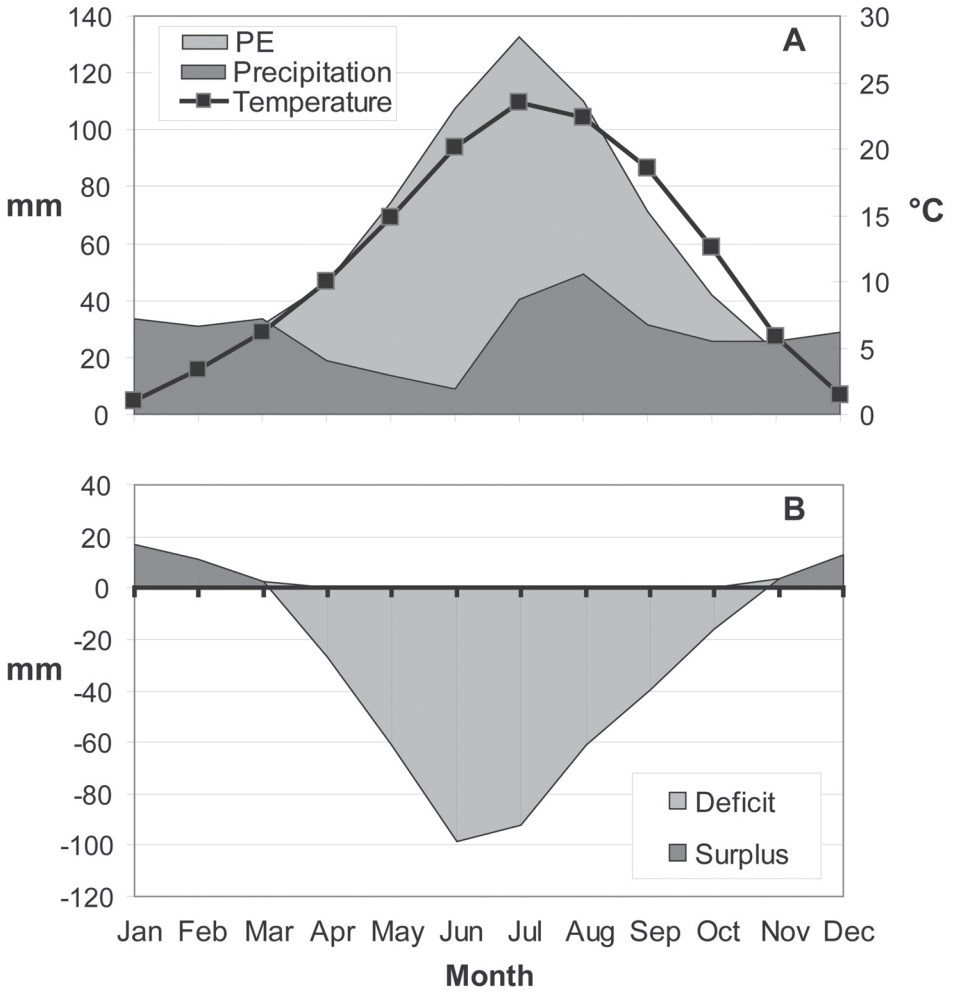


**Figure 2.** Southern Colorado Plateau moisture balance. (A) Mean monthly temperature, precipitation, and potential evapotranspiration (PE) for 1950–1999. (B) Precipitation minus potential evapotranspiration. Potential evapotranspiration is calculated using Hamon's method (Hamon 1961). Data: PRISM 4 km (Daly et al. 1994); PE calculations provided by Andrew Ellis, Arizona State University.

plant species allow them to take advantage of seasonal patterns in available moisture. Topographic diversity within northern Arizona creates several vegetation life zones within the region. Temperature and precipitation can vary greatly from the lower regions of the Grand Canyon to the top of the San Francisco Peaks, but the seasonality of these parameters is the same, regardless of altitude, slope, and aspect. Annual precipitation follows a bimodal distribution, split between large, spatially coherent, winter frontal storms and isolated summer monsoon convective storms.

Moisture surplus in the SCP typically occurs from November to March (Figure 2). April reflects a turning point when monthly mean temperatures rise to a point where the

growing season typically begins even as precipitation decreases. By May and June, temperatures rise high enough to affect water vapor pressure. The typically sparse rainfall does little to offset high levels of potential evapotranspiration (PE). This period of time can cause severe vegetation stress and even mortality in seedlings lacking an established root system and, during extreme years, in established perennial species (Breshears et al. 2005). Many of the perennial bunch grasses common to northern Arizona remain semi-dormant during this time period. For woody plant recruitment, this is often a critical period; ponderosa pine (*Pinus ponderosa)*, the dominant tree in the region, has been shown to have had cohort events occurring during anomalously cool and wet May–June periods (Savage et al. 1996). Conversely, ponderosa forests are most susceptible to damage from infestions of bark-beetle (primarily *Dendroctonus* spp. and *Ips* spp.) and wildfires when these pre-monsoon months are anomolously dry (Adams et al. 2009).

On average, Southern Colorado Plateau summer monsoon precipitation begins in mid-July (Higgins et al. 1999). Although it occurs during a time when PE and average monthly temperature are at their annual peaks, it typically brings enough precipitation to decrease the moisture deficit during this time of year (Figure 2). As average monthly temperature begins to decrease in August, monsoon precipitation reaches its regional apex, which further decreases the moisture deficit. By mid-September, monsoon precipitation typically decreases, but so does temperature. October, like April, is a transition period between annual moisture surplus and deficit.

In the rest of this chapter, we describe the process of GCM selection and statistical downscaling of climate parameters, and the implications of these results. In the introduction, we describe the GCM data, downscaling methods, and model-selection criteria. In the data and methods section we discuss the GCMs and ensemble averages selected, and we examine the spatial and temporal fidelity of the GCMs in reproducing the seasonal cycle of temperature and precipitation over the study domain, the Southern Colorado Plateau. In the section on the results of model selection and simulations of Colorado Plateau seasonal cycle, we discuss the GCM projections for the twenty-first century over the study domain. In the discussion section, we consider implications for colleagues interested in vegetation modeling and alternatives to our approach that may inform future studies. The final section contains a summary of major conclusions.

## DATA AND METHODS

### Historic Climate Records

To compare historic observations to GCM simulations, in order to correct model biases and implement downscaling algorithms, we used mean monthly temperature and monthly total precipitation data from the Parameter-elevation Regressions on Independent Slopes Model (PRISM) 4 km grid cell resolution dataset (Daly et al. 1994) (www.prism.oregonstate.edu). PRISM uses point data, spatial data sets, a knowledge base, and expert interaction to generate estimates of gridded monthly climatic parameters (Daly et al. 2001). A combination of linear regression and a series of rules, decisions, and calculations set weights for the station data entering the linear regression (Daly et al. 2002). The weighting function contains information about relationships between the climate field and geographic or meteorological factors. Weighting factors include measures such as elevation, distance from the predicted location, station clustering, vertical layer (to account for local inversions), topographic facet (to account for rainshadows), coastal proximity, and effective terrain weights (Daly et al. 2002). We compared PRISM estimates to simulations for the period

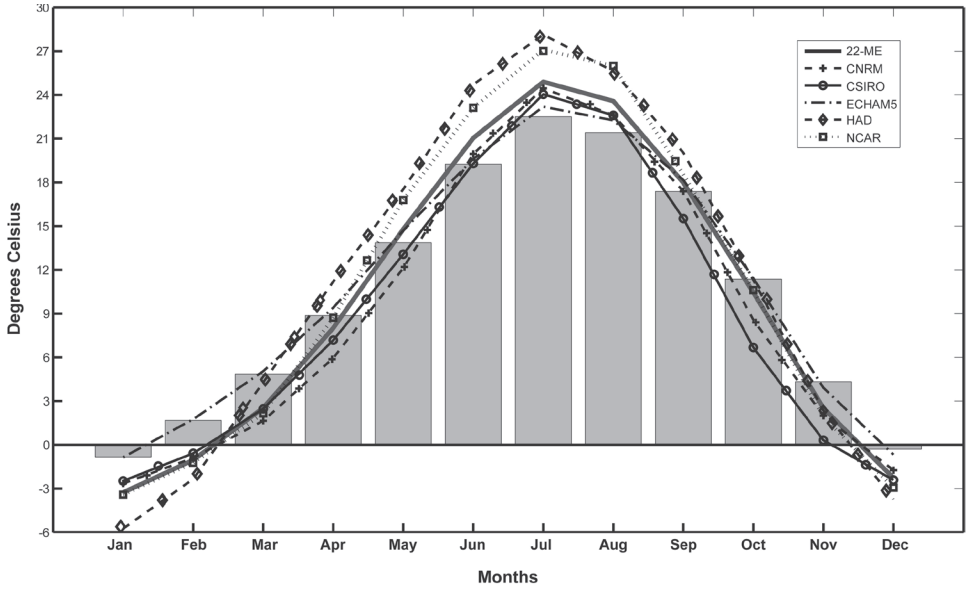


**Figure 3.** Southern Colorado Plateau observed (bars) and GCM simulated (lines) mean monthly temperature (°C), 1950–1999. See Table 1 for GCM acronyms. "22-ME" refers to the ensemble mean of 22 GCMs used in the IPCC Fourth Assessment Report data set (Meehl et al. 2007). Observed data: PRISM 4 km (Daly et al. 1994).

1895–2000 (used in Figures 3–9), and used 1950–1999 as the climatological average period for calculating anomalies. PRISM provides the most topographically precise, methodologically sound, quality-controlled historic climate data set available for century-long time scales; thus, PRISM is a robust choice for spatial and topographic concerns that underlie the requirements of vegetation models that will be served by downscaled GCM projections from this study.

### Global Climate Model (GCM) Projections

We garnered climate model projections used in the Fourth Assessment Report (AR4) of the Intergovernmental Panel on Climate Change (IPCC) from the Program for Climate Model Diagnosis and Intercomparison (PCMDI) archive. Details on the models and their configurations are available at *http://wwwpcmdi.llnl.gov/ipcc/about ipcc.php*. These projections used coupled ocean-atmosphere models (AOGCMs) to simulate climate variations spanning the late nineteenth century to the end of the twenty-first century (see Meehl et al. 2007); this generation of models is referred to as Coupled Model Intercomparison Project version 3 (CMIP3). We analyzed, individually, 22 of these models (48 simulations; Table 1) that are forced with estimated greenhouse gas and aerosol changes from the late nineteenth century through 1999, and the IPCC Special Report on Emissions Scenarios (SRES) A1B scenario from 2000 to 2100. The A1B scenario describes a future world of rapid economic growth, with global population that peaks in mid-century then declines, and rapid introduction of new and more efficient technologies that are balanced such that no single source of energy is overly dominant (Nakicenovic et al. 2000). This scenario, sometimes referred to as "the medium non-mitigation scenario" (Moss et al. 2008), has

**Table 1.** GCM rankings for spatial correlation between GCM simulation and observed seasonal precipitation over land in the western United States, 1950–1999. Low rank indicates the best combined correlations with the annual cycle of precipitation. **Bold** font indicates GCM identifiers used in the text.

| GCM | Modeling Center, Country | Rank |
|---|---|---|
| **HAD**GEM1 | Hadley Centre, UK | 10 |
| **ECHAM5**/MPI | Max Planck Institute, Germany | 26 |
| ECHAM4/MPI | Max Planck Institute, Germany | 27 |
| CGCM3.1/T63 | Canadian Centre for Climate Modelling & Analysis | 29 |
| GFDL-CM2.1 | NOAA Geophysical Fluid Dynamics Lab, US | 35 |
| CGCM3.1/T47 | Canadian Centre for Climate Modelling & Analysis | 37 |
| GISS-EH | NASA Goddard Institute for Space Studies, US | 37 |
| HadCM3-UKMO | Hadley Centre, UK | 38 |
| MIROC3.2(medres) | Center for Climate System Research (The University of Tokyo), National Institute for Environmental Studies, and Frontier Research Center for Global Change (JAMSTEC), Japan | 39 |
| **CNRM** CM3 | Météo-France / Centre National de Recherches Météorologiques, France | 42 |
| **CSIRO** MK3.0 | CSIRO, Australia | 42 |
| MIROC 3.2(hires) | Center for Climate System Research (The University of Tokyo), National Institute for Environmental Studies, and Frontier Research Center for Global Change (JAMSTEC), Japan | 44 |
| MIUB ECHO-G | Meteorological Institute of the University of Bonn, Meteorological Research Institute of KMA, and Model and Data group. | 50 |
| **NCAR** CCSM3 | National Center for Atmospheric Research, US | 50 |
| GISS-ER | NASA Goddard Institute for Space Studies, US | 53 |
| NCAR PCM1.0 | National Center for Atmospheric Research, US | 56 |
| BCCR BCM2.0 | Bjerknes Centre for Climate Research, Norway | 58 |
| GFDL-CM2.0 | NOAA Geophysical Fluid Dynamics Lab, US | 62 |
| GISS-AOM | NASA Goddard Institute for Space Studies, US | 63 |
| IAP-FGOALS | Institute of Atmospheric Physics, People's Republc of China | 67 |
| ISPL-CM4 | Institut Pierre Simon Laplace, France | 71 |
| INM-CM3.0 | Institute for Numerical Mathematics, Russia | 76 |

been favored for analyses in some situations where capturing the full range of scenario output may be too computationally intensive (*sensu* Seager et al. 2007). It is known by some as the "business as usual" scenario and, as such, is a reasonable choice of emission scenario for examining plausible futures. Further, all the scenarios yield similar output

through about 2030. It is only after mid-century that the scenarios begin to diverge extensively. We analyzed total monthly precipitation and monthly mean temperature for each individual model and the 22-model ensemble mean (Hoerling et al. 2007).

### Downscaling

The AR4 GCMs use a variety of grid resolutions, typically in the range of approximately 2.5° (~300 km in middle latitudes) per side of the grid box. The first step in the data treatment is to align the GCMs to a common grid, in this case to the same 4 km grid used by PRISM, using inverse distance weighting (Eischeid et al. 2000). Once the GCM estimates for each parameter have been re-gridded, we statistically downscale the GCM estimates using the method described in detail by Salathé (2005) and summarized in this section. The method uses the PRISM estimates to impose spatial structure to the GCM-simulated monthly precipitation and temperature, while preserving the atmospheric processes driving the simulations. As mentioned by Salathé (2005), Widmann et al. (2003) used a similar method, referred to as "local scaling."

To remove the bias between the large-scale simulated climate parameter and the observed climate parameter at each grid cell, we apply monthly corrections so magnitudes of the GCM simulations of the historic period conform to observations for the 1950–1999 period of overlap with the PRISM data. The twentieth-century runs used to fit each model are simulations forced by historic variations in greenhouse gases, solar output, and atmospheric aerosol loading. For each of the models presented here, the twentieth-century runs were obtained from the PCMDI archive. The aforementioned biases are presumed to be the same from year to year, because at the monthly time scale the models can resolve the large-scale weather systems that generate observed temperature and precipitation across the Colorado Plateau. The spatial biases and magnitudes are corrected independently at each grid point for each model, by multiplying the simulated parameters by monthly bias factor (for precipitation) or by taking the difference between the simulation and the bias factor (for temperature), as described with the equations adapted from Salathé (2005) below.

Let $P_{mod}(x, t)$ be the simulated monthly precipitation for the large-scale gridpoint in location x and at time t (in months); $(P_{mod})_{mth}$ is the monthly mean taken over the period of overlap between the simulated data and observations $(P_{obs})_{mth}$. The downscaled monthly mean precipitation ($P_{ds}$), then, can be calculated by:

$$P_{ds}(x,t) = P_{mod}(x,t)\,(P_{obs})_{mth}/(P_{mod})_{mth}$$

The fitting is performed independently for each month.

Surface air temperature is downscaled in a similar way. For temperature, the adjustment uses the difference between the mean bias and the observations. Let $T_{mod}(x, t)$ be the simulated monthly temperature, $(T_{mod})_{mth}$ be the simulated monthly mean taken over the fitting period, and $(T_{obs})_{mth}$ be the monthly mean of the observations taken over the fitting period. Then, the downscaled monthly mean surface temperature ($T_{ds}$) can be calculated by:

$$T_{ds}(x,t) = T_{mod}(x,t) + [(T_{obs})_{mth} - (T_{mod})_{mth}]$$

This correction assumes that the large-scale temperature predicts the local temperature, given the removal of a monthly bias in the mean. Salathé (2005) notes that this additive methodology may be thought of as a lapse-rate correction due to the elevation difference of the local gridpoint relative to the GCM grid. Like Salathé, we make no allowance for possible changes in the lapse rate as a consequence of climate change. Despite these limitations to the aforementioned methods, and the dependency of this statistical approach on the accuracy

of the regional circulation patterns produced by the GCMs (CCSP 2008), the method is computationally efficient, and previous studies show a relatively high confidence in the simulations of storms and jet streams in the middle latitudes (CCSP 2008).

### Ranking procedure

In order to determine the most appropriate GCMs to use in the vegetation change analyses, we ranked the models using four metrics based on the fit between the GCM climatological estimates of western U.S. seasonal precipitation during the period of fit and the observed seasonal precipitation averaged over the period 1950–1999. We compared observed parameters and GCM projections for three seasons chosen for their influence on Colorado Plateau vegetation: November–March (winter), May–June (pre-monsoon) and July–September (monsoon). We did not assess fit between simulated and observed temperature, because it is well known that there is good agreement between model temperature simulations for western North America (IPCC 2007), and the bias corrections should account for differences in magnitude. We acknowledge that, compared with temperature, spatial variations in precipitation are less well understood and that there is a greater spread between models in simulated precipitation—thus, choice of models can make a difference in the application of projections for decision-making (IPCC 2007; CCSP 2008; Brekke et al. 2008). We assume that models that simulate well the recent precipitation history of these key seasons are likely to simulate key characteristics of future climate—although Pierce et al. (2009) found no strong relationship between the score of the CMIP3 models on a set of performance metrics and the results of a detection and attribution study of western North America temperatures. In using this metric, we acknowledge that we cannot tell whether well-fitting simulations for our region produce the "right results" for the wrong (mechanistic) reasons.

We computed four values for each model, using metrics computed seasonally and then averaged, for the evaluation domain of interest, the continental United States west of 100°W. We evaluated the models based on this western-U.S. comparison rather than the much smaller domain of our study area in order to encompass a larger array of grid points in the GCMs. We reasoned that if the models cannot perform well for the West as a whole, their performance in our study area could be the result of chance rather than skill. The values we computed are as follows:

- the spatial correlation coefficient between simulated and observed (PRISM) precipitation at the 4 km scale over the domain of interest for each of the three selected seasons;
- the spatial congruence coefficient for the same;
- the mean ratio of simulated/observed area-averaged precipitation for each 4 km grid cell over the domain of interest, based on the seasonal precipitation totals in millimeters; and
- the mean ratio of simulated/observed area-averaged precipitation for each 4 km grid cell over the domain of interest, based on the seasonal precipitation expressed as a percentage of the annual total.

These metrics evaluate the GCMs' fidelity for spatial distribution of precipitation, precipitation amplitude, and seasonal cycle of precipitation. These four sets of metrics for each of the 22 models were then ranked, and the ranks summed for each model. The best rank for each metric is 1, and the worst is 22. The best possible cumulative rank is 4, i.e., a rank of 1 for each of the four metrics. For example, the HAD model produced the following ranks: 1, 3, 3, 3, which yielded an overall score of 10 (Table 1).

We acknowledge that the GCMs differ significantly in terms of basic physical and

dynamical design and number of atmospheric and oceanic layers; accounting for such factors may have resulted in a different choice of models. For example, process-based measures, such as the ability of a model to reproduce the El Niño-Southern Oscillation (ENSO), are certainly appropriate for studying Colorado Plateau climate; however, a model with acceptable ENSO simulation may lack acceptable monsoon simulation. Although several studies project decreasing annual precipitation in the southwestern United States (IPCC 2007, Seager et al. 2007), we recognize the limitations of statistically downscaling GCM output to our study area. As we show below, the annual cycle of precipitation for the western United States is poorly simulated by many of these models (Pierce et al. 2009), a result also found in studies of previous generations of models (Coquard et al. 2004).

## RESULTS: MODEL SELECTION AND SIMULATIONS OF COLORADO PLATEAU SEASONAL CYCLE

GCMs were ranked based upon their performance in the western half of the United States, using fidelity to seasonal and spatial statistics of precipitation as the overarching metric (Table 1). The overall score for the HAD model (10) produced the lowest rank of all models used in this analysis—that is, HAD precipitation for 1950–1999 was most faithful to the seasonal cycle and spatial distribution of precipitation in the observed record. The next closest score was 26 (ECHAM5). For each of the four ranking metrics, the order of models (best/lowest to worst/highest) did not change much (not shown). In other words, any of the above four metrics individually produce approximately the same order as that for summing the four and then ranking the models.

Rank results did not form the final basis for model selection, although all GCMs selected did rank in the top 11, accounting for ties in some of the rankings (Table 1). Along with the top two models, three other models were selected, based on subjective criteria. CSIRO (score 42) and CNRM (score 42), which tied for rank 9, were included because together they bracket the range of published projections for aridity in the southwestern United States (Seager et al. 2007). Seager and his colleagues modeled precipitation minus evaporation anomalies (P-E) using A1B-emissions scenario projections for 19 IPCC AR4 models. Mid-century (2041–2060) projections ranged from about -0.12 mm/day (CNRM) to no detectable change; CSIRO and HAD both showed near zero change or slight increases in P-E (Figure 2 of Seager et al. 2007). NCAR (score 50; rank 11) was selected because of opportunities to use this model to expand upon this work in collaboration with other investigators (e.g., Govindasamy et al. 2003, Diffenbaugh et al. 2005). None of these five models required flux corrections in order to maintain a stable climate in control runs (Kripalani et al. 2007).

A 22-model ensemble mean (22-ME) also was included for comparison with the individual models. Ensemble means generally improve the performance of climate simulations at both global (Reichler and Kim 2008) and regional scales (Pierce et al. 2009). Pierce and colleagues (2009) compared 42 performance metrics on 21 current GCMs and found multimodel ensemble means consistently outperformed individual models used for a climate change detection and attribution study. They found that a suite of at least five randomly selected models proved superior to any individual model, as long as at least 14 model runs were incorporated, because ensembles with sufficient realizations reduce the effects of internal climate variability. (N.B.: in this and other analyses, multiple realizations of models are included when available). They traced the improved performance of multimodel ensembles to the cancellation of offsetting errors in the individual models. These results

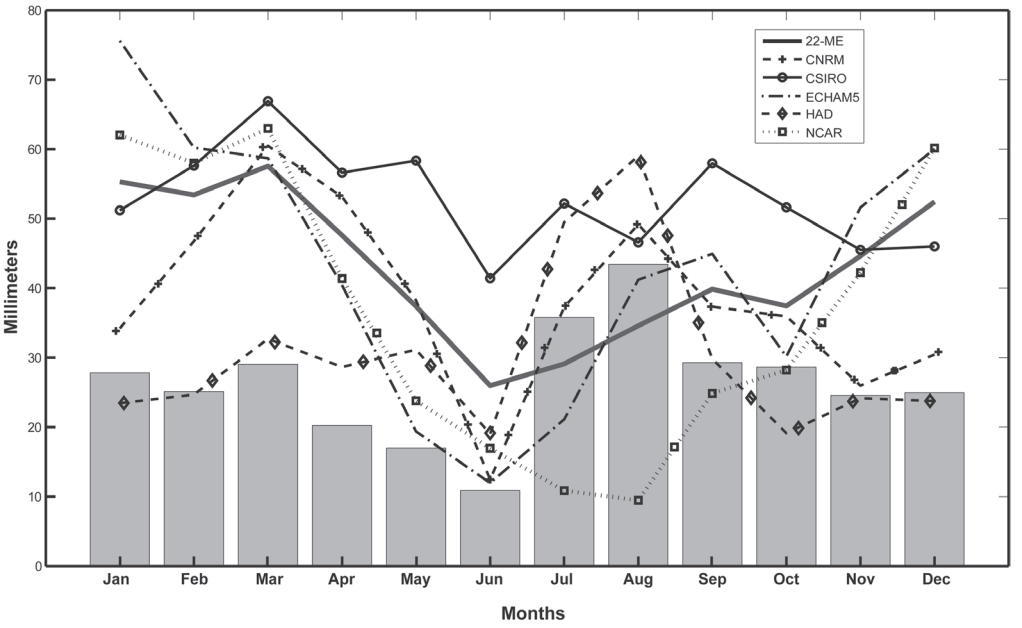


**Figure 4.** Southern Colorado Plateau observed (bars) and GCM simulated (lines) mean monthly precipitation (mm), 1950–1999. See Table 1 for GCM acronyms. "22-ME" refers to the ensemble mean of 22 GCMs used in the IPCC Fourth Assessment Report data set (Meehl et al. 2007). Observed data: PRISM 4 km (Daly et al. 1994).

were robust, regardless of whether the "best" models, based on comparisons with historical data, were selected. However, by defining the mean more precisely through a larger sample size, ensemble mean results display less interannual variability than individual models. For the purpose of ecological studies, which are dependent on the interannual variability in time series, it is often the extremes rather than the average conditions that define the boundaries of species distribution. Consequently, in this paper, emphasis will also be given to the individual model results.

### Simulations for Southern Colorado Plateau area

The GCMs more closely simulate the seasonal cycle of 1950–1999 Colorado Plateau monthly mean temperature than they simulate the seasonal cycle of monthly mean precipitation (Figures 3 and 4). This is consistent with results from global-scale studies; Covey et al. (2003) found that historic global temperatures generated by CMIP2-coupled atmosphere-ocean Global Climate Models (AOGCMs) correlated exceedingly well with historic observed temperatures ($r > 0.93$ for each model), whereas correlations between AOGCMs and observed precipitation ranged from 0.4 to 0.7.

### Temperature

The ECHAM5 model shows the closest match to the observed seasonal cycle of Colorado Plateau temperatures (Figure 3). HAD exaggerates the seasonal temperature range; HAD temperatures are too hot in summer and too cold in winter. The NCAR model shows a similar exaggeration of average monthly temperature range. The CNRM and CSIRO models exhibit seasonal cycles similar to the ensemble average—temperatures that are

**Table 2.** Observed and simulated temperature (top) and precipitation (bottom) for the three seasons analyzed in this study (November–March; May–June; July–September). See Table 1 for GCM acronyms. "22-ME" refers to the ensemble mean of 22 GCMs used in the IPCC Fourth Assessment Report data set (Meehl et al. 2007). Observed data: PRISM 4 km (Daly et al. 1994). Temperature is in °C. Precipitation is in mm.

| TEM | PRISM | CNRM | ECHAM5 | NCAR | CSIRO | HAD | 22-ME |
|---|---|---|---|---|---|---|---|
| NOV-MAR | 2.0 | -0.3 | 1.8 | -0.7 | -0.5 | -1.0 | -0.3 |
| MAY-JUN | 16.6 | 16.0 | 17.2 | 20.0 | 16.2 | 21.1 | 17.9 |
| JUL-SEP | 20.4 | 21.5 | 21.2 | 23.9 | 20.7 | 24.6 | 22.1 |
| **PRECIP** | **PRISM** | **CNRM** | **ECHAM5** | **NCAR** | **CSIRO** | **HAD** | **22-ME** |
| NOV-MAR | 131.5 | 197.9 | 306.2 | 285.5 | 267.3 | 128.8 | 263.4 |
| MAY-JUN | 27.9 | 50.7 | 31.3 | 40.8 | 99.8 | 50.2 | 63.4 |
| JUL-SEP | 108.5 | 123.8 | 107.3 | 45.2 | 156.8 | 138.4 | 103.6 |

cooler than the observed average during the winter, spring, and fall months, but near the observed average during the summer months. The IPCC Fourth Assessment Report notes that Western North America temperature was underestimated by most AR4 GCMs (Christensen et al. 2007); the median bias for annual temperature was -1.3°C. The most pronounced under-estimation of seasonal temperature was for spring (March–May); the median bias was -2.0°C.

### Precipitation

HAD shows the best match with the observed seasonal cycle of precipitation (Figure 4) and associated spatial distribution of precipitation (Table 3). Although HAD projections for July and August total precipitation are 38.3% and 36.0% higher, respectively, than the observed, it is the only model considered here that does not drastically overestimate Colorado Plateau winter season precipitation (Figure 4; Table 2). The NCAR model depicts a Mediterranean climate seasonal cycle of precipitation for the Southern Colorado Plateau region, whereas the CSIRO shows little variation in precipitation between months, in contrast to the observed bimodal season cycle. The CNRM, ECHAM5 and the 22-ME all show bimodal seasonal cycles, but overestimate November–March precipitation, as well as April and September precipitation.

Table 3 presents a qualitative comparison of model estimates versus observed precipitation for the Southern Colorado Plateau (SCP). For November–March, most of the models overestimate SCP mean precipitation. The HAD and 22-ME produce wetter than observed conditions in the southeastern quadrant of the SCP. The CSIRO, ECHAM5, and NCAR models all exhibit wetter than observed winter precipitation, with the ECHAM5 showing more than double the observed precipitation over most of the SCP domain. The CRNM CM3 simulates wetter than observed precipitation over the southern half of the SCP. Overestimation of winter precipitation in the U.S. West is a long-standing issue

**Table 3.** Qualitative assessment of GCM simulated precipitation compared to observations (1950–1999) for the Southern Colorado Plateau (SCP; see Figure 1). Each bold outlined box represents the SCP, and each quadrant of a bold outlined box represents one quadrant of the domain, corresponding to Figure 1 (clockwise from left, NW NE, SE, SW). Sign indicates the direction of projection, boldness indicates magnitude. **+** much greater than observed; + greater than observed; – less than observed; **—** much less than observed. Blanks indicate approximately similar total precipitation.

| Model | Winter PPT (Nov-Mar) | | Spring PPT (May-Jun) | | Summer PPT (Jul-Sep) | |
|---|---|---|---|---|---|---|
| 22-Model Ensemble | | | + | **+** | – | + |
| | | + | | + | – | + |
| UKMO-HADGEM1 | | | | + | – | + |
| | | + | | + | – | + |
| MPI-ECHAM5 | **+** | | | | – | + |
| | **+** | **+** | | | – | + |
| CSIRO-MK3 | + | + | + | **+** | | **+** |
| | + | **+** | + | **+** | – | **+** |
| CNRM-CM3 | | | | + | – | + |
| | + | **+** | | + | – | **+** |
| NCAR-CCSM3 | **+** | + | | + | – | – |
| | + | **+** | | + | **—** | – |

among GCMs (Coquard et al. 2004), related in part to the complex topography of the region (Duffy et al. 2003). The IPCC Fourth Assessment Report notes that more than 75% of the models overestimated western North America annual and seasonal precipitation (Christensen et al. 2007). The median precipitation bias was highest for winter (93%, December–February) and lowest for summer (28%, June–August); the median annual precipitation bias was 65%.

For May–June, with the exception of the ECHAM5, all models and the 22-ME produce wetter than observed precipitation in the eastern half of the SCP. In particular, the CSIRO model produces well more than double the observed precipitation in the eastern half of the SCP. For July–September, the differences between models and observations are even more pronounced, with most models showing greater than observed precipitation in the eastern half of the SCP and less than observed precipitation in the western half of the SCP. Similar to the spring season, the CSIRO model produces double the observed summer precipitation

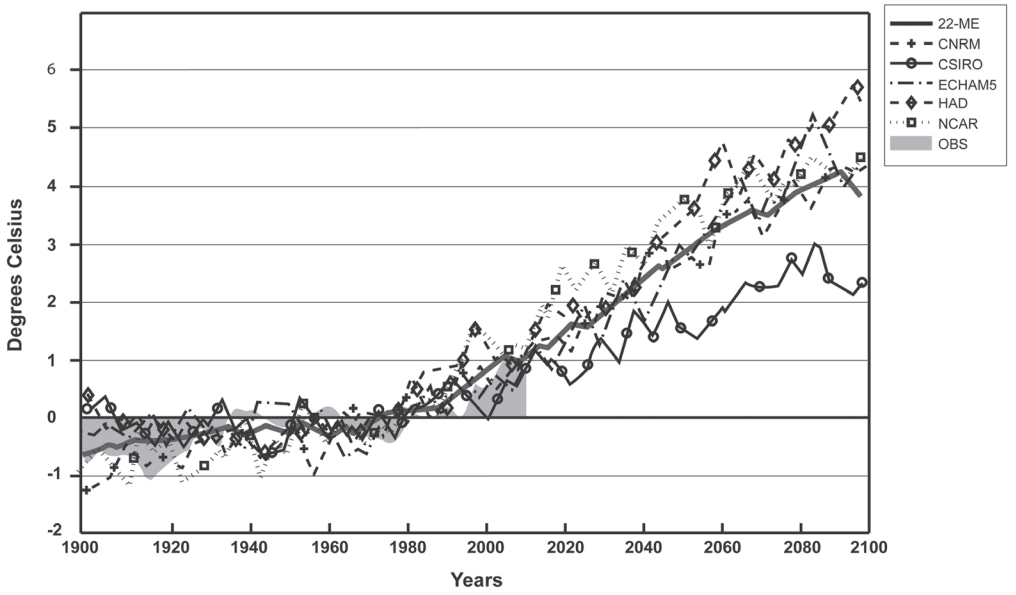


**Figure 5.** Southern Colorado Plateau observed (shaded) and GCM projected (lines) mean annual temperature (°C). See Table 1 for GCM acronyms. "22-ME" refers to the ensemble mean of 22 GCMs used in the IPCC Fourth Assessment Report data set (Meehl et al. 2007). Observed data: PRISM 4 km (Daly et al. 1994).

in the eastern half of the SCP; as mentioned above, the CSIRO model does not produce a strong seasonal cycle, and overestimates precipitation in every single month (Figure 4). The NCAR model produces conditions drier than observed over the entire SCP domain. A study by Lin et al. (2008) determined that most of the AR4 models overestimate precipitation in the core monsoon region and fail to show the monsoon retreat.

In the section above, we described the biases in the models and their general correspondence with the seasonal cycles of temperature and precipitation, as well as the spatial distribution of precipitation in the SCP. As mentioned in the Data and Methods section, the monthly bias between the GCM and observed estimates is removed independently at each grid cell. We assume that each model's bias, based on simulations, remains consistent in projections of future conditions; thus correcting this bias should yield more reasonable projected values. Nevertheless, it is valuable to reflect on model bias when interpreting the downscaled projections presented in the next section.

## RESULTS: MODEL PROJECTIONS FOR THE SOUTHERN COLORADO PLATEAU

Projections for the SCP all show increasing temperatures after 1980 (Figure 5). When the 22 model projections are averaged together (22-ME), the temperature increase appears to be nearly monotonic, reaching 2.2°C above the observed average in the 2030s, and 4.0°C above the observed average by the end of the century. Individual models exhibit considerable multi-year variability within the upward trends in temperature. With the exception of the CSIRO model, which projects a considerably lower temperature increase of 2.3°C by the end of the century, individual models selected for this study show increases comparable to the

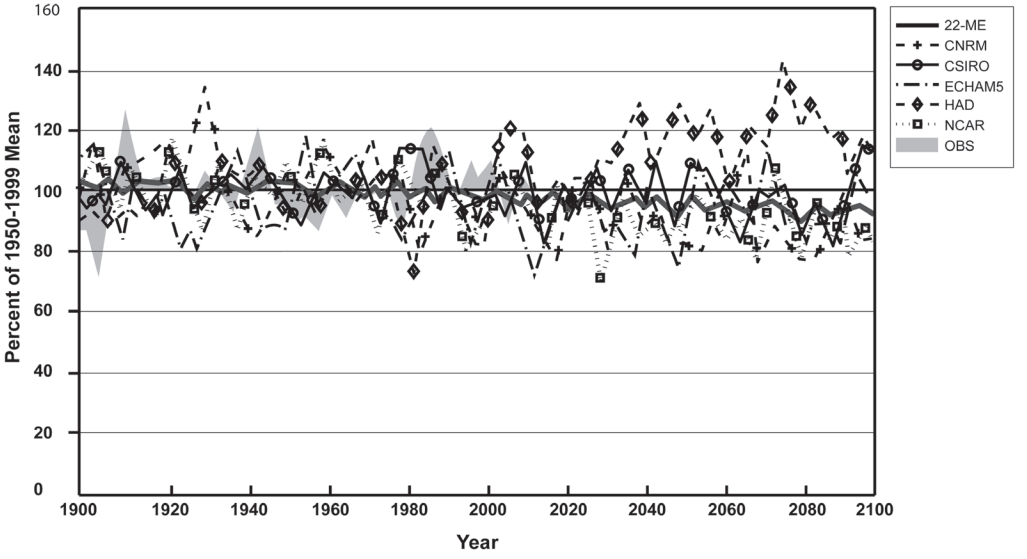


**Figure 6.** Southern Colorado Plateau observed (shaded) and GCM projected (lines) mean annual precipitation (mm). See Table 1 for GCM acronyms. "22-ME" refers to the ensemble mean of 22 GCMs used in the IPCC Fourth Assessment Report data set (Meehl et al. 2007). Observed data: PRISM 4 km (Daly et al. 1994).

22-ME. HAD projects the greatest annual temperature increases, reaching 5.4°C above the observed average by 2080.

Seasonal temperature projections (not shown) exhibit slightly higher rates of increase for the arid foresummer and summer seasons than for the cool season. The 22-ME projection for the SCP warm seasons reaches 2.5°C above the observed average in the 2030s, and 4.7°C higher than observed average values by the end of the century. November–March seasonal temperature projections reach 1.9°C above the observed average by 2040, and 3.6°C above the average by the end of the century. In all seasons, the CSIRO shows lower temperature increases than the other models. The HAD projects much higher winter temperature increases than the other models (6.0°C higher than average by the end of the century) and, probably due to its exceedingly high projection of July–September precipitation, less than the 22-ME mean increase during the summer. The NCAR, which characterizes the SCP as having a Mediterranean seasonal precipitation cycle for 1950–1999, projects the greatest summer season temperature increases (4.8°C by the end of the century). Timbal et al. (2008) found the CSIRO model the least sensitive (2.11°C) and the ECHAM5 most sensitive (3.69°C) models when comparing the global temperature sensitivity of 10 AR4 GCMs modeling the A1B scenario for the twenty-first century. The HAD was not among the models tested, but similar to this study, CNRM temperature sensitivity was roughly in the middle (2.81°C).

SCP precipitation projections show a wide range of possibilities, and few coherent trends. This is not surprising, and is consistent with the CCSP (2008) and IPCC (2007) statements that AOGCMs are often not reliable for simulating sub-continental scale precipitation. The 22-ME projection suggests a slight decline (6.5%) in annual precipitation for the Colorado Plateau (Figure 6). Most of the GCMs we

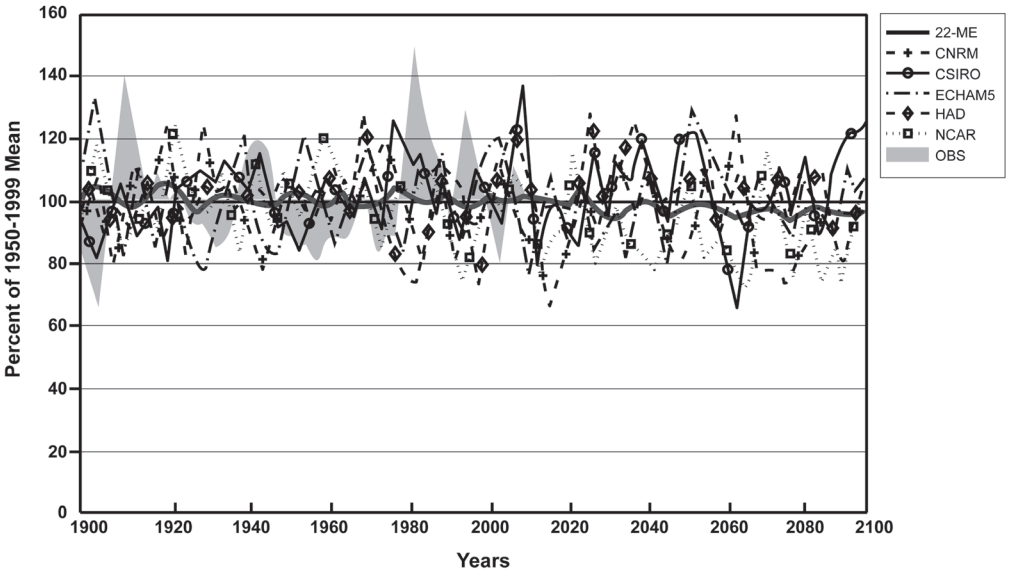


**Figure 7.** Southern Colorado Plateau observed (shaded) and GCM projected (lines) mean November–March total precipitation (mm). See Table 1 for GCM acronyms. "22-ME" refers to the ensemble mean of 22 GCMs used in the IPCC Fourth Assessment Report data set (Meehl et al. 2007). Observed data: PRISM 4 km (Daly et al. 1994).

selected project annual precipitation below the observed 1950–1999 average for most of the twenty-first century. Most models show decade-scale variations, with few pluvials of the magnitude seen during the twentieth century. HAD, however, projects higher than observed mean SCP precipitation for most of the twenty-first century, due to several decade-scale winter pluvials, and an overall increase in summer precipitation, averaging 50% above observed after 2040 (Figures 6–9). SCP November–March precipitation projections indicate great variability between models and no strong trends (Figure 7); the 22-ME projects a slight decline in winter precipitation of about 5% during the course of the century.

SCP May–June precipitation projections agree on mostly below-observed-average precipitation during the course of the twenty-first century, with some substantial differences in multi-decade variability and the magnitude of declining arid foresummer precipitation (Figure 8). In particular, the 22-ME declines throughout the century, averaging about 75% of climatology during the last decades of the century. The CNRM projects the greatest decline in SCP May–June precipitation (47.8%, with an average of 50% lower than climatology for the last three decades of the century). The CSIRO projects consistently below-average SCP May–June precipitation, reaching about 25% below climatology by the last few decades of the century (Figure 8).

SCP July–September precipitation projections also indicate great variability between models and no clear trends; the 22-ME projects a slight increase in summer precipitation during the course of the century, modulated by multi-decadal variability (Figure 9). The HAD model shows a clear and dramatic increase in SCP summer precipitation after 2020, with regional totals far in excess of observations. On the other hand, the ECHAM5 model projects mostly below-observed-average SCP summer precipitation during the twenty-first century.

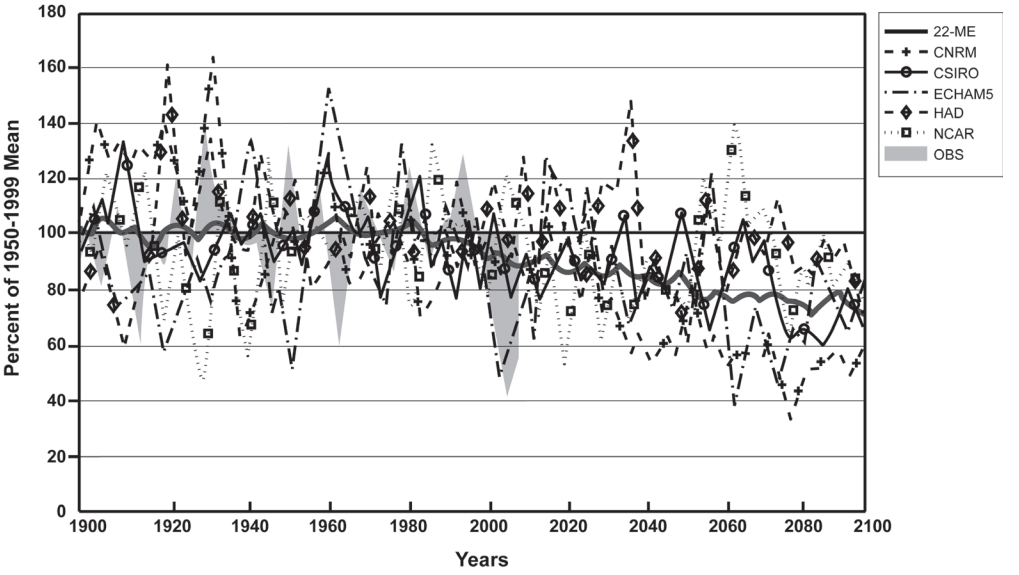


**Figure 8.** Southern Colorado Plateau observed (shaded) and GCM projected (lines) mean May–June total precipitation (mm). See Table 1 for GCM acronyms. "22-ME" refers to the ensemble mean of 22 GCMs used in the IPCC Fourth Assessment Report data set (Meehl et al. 2007). Observed data: PRISM 4 km (Daly et al. 1994).

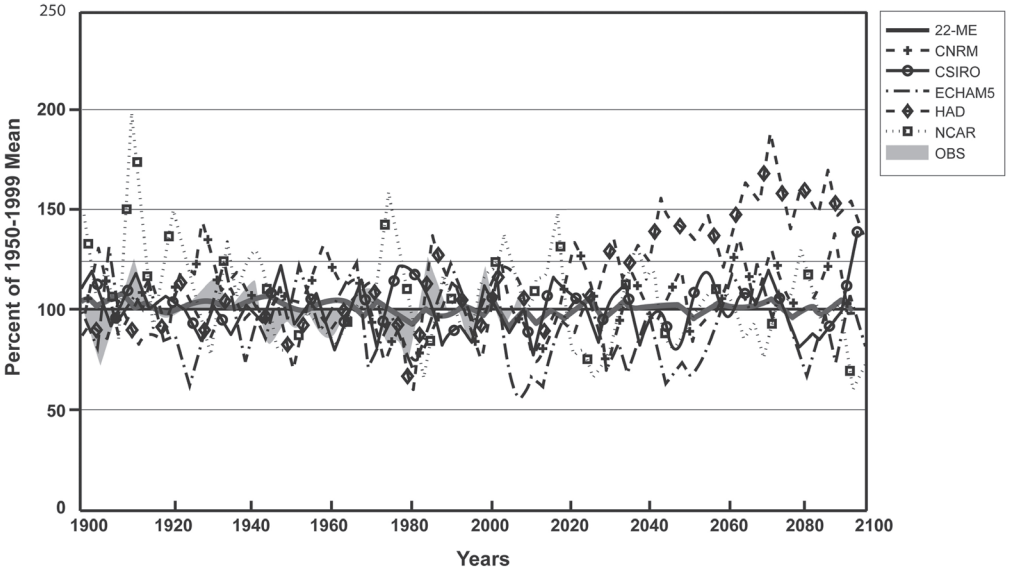


**Figure 9.** Southern Colorado Plateau observed (shaded) and GCM projected (lines) mean July–September total precipitation (mm). See Table 1 for GCM acronyms. "22-ME" refers to the ensemble mean of 22 GCMs used in the IPCC Fourth Assessment Report data set (Meehl et al. 2007). Observed data: PRISM 4 km (Daly et al. 1994).

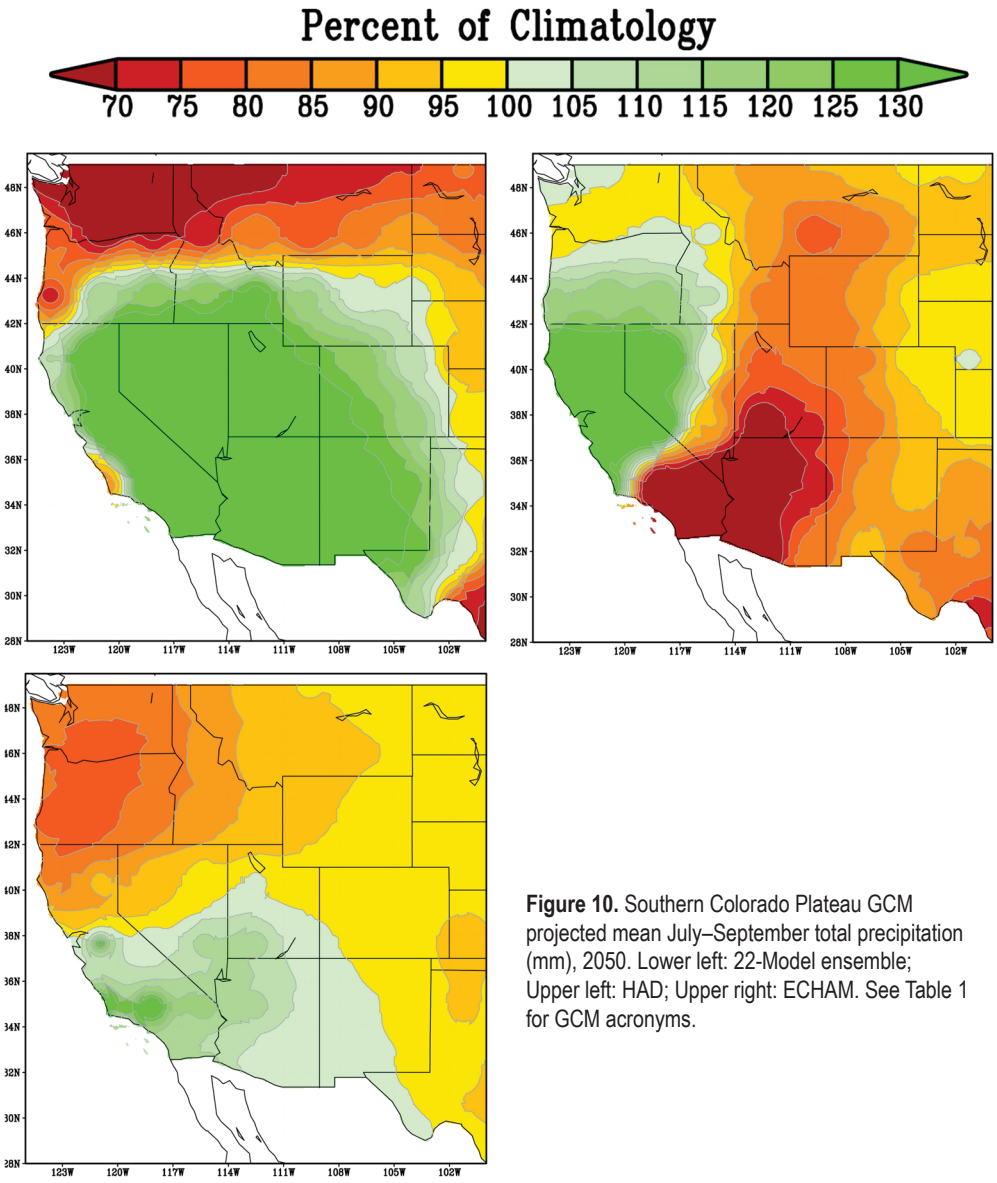


**Figure 10.** Southern Colorado Plateau GCM projected mean July–September total precipitation (mm), 2050. Lower left: 22-Model ensemble; Upper left: HAD; Upper right: ECHAM. See Table 1 for GCM acronyms.

In this study, the two top-ranking GCMs, based on their skill in simulating observed-average precipitation in the West (HAD and ECHAM5, Table 1), project radically different precipitation changes in the mid-century example considered; this is particularly the case for summer precipitation (Figure 10; Table 4). For mid-century July–September precipitation, the HAD projects a 30% increase for the Colorado Plateau area, whereas the ECHAM5 projects a comparable decrease for the western three-fourths of the domain (Table 4). For May–June mid-century precipitation (Table 4), the two

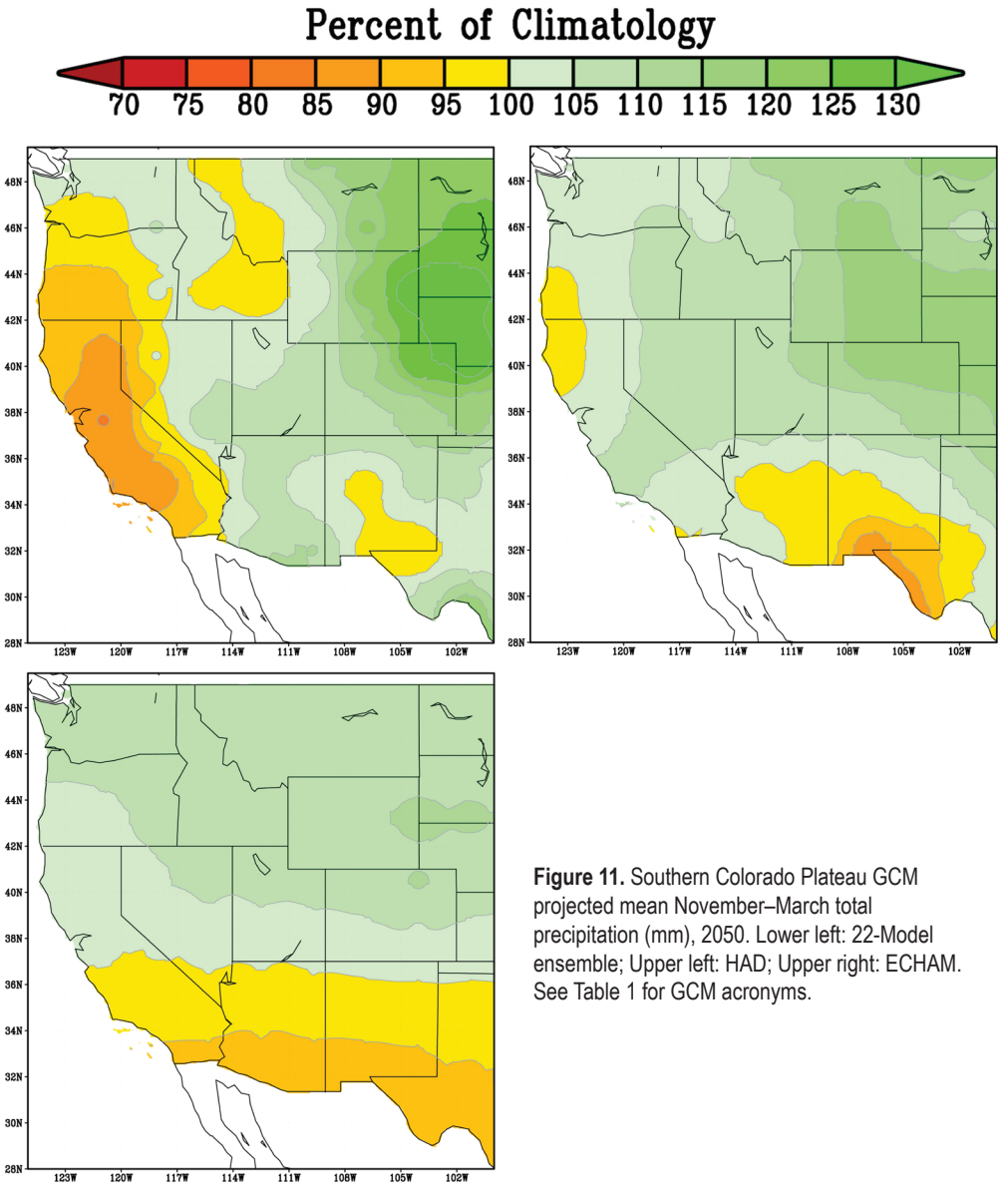


**Figure 11.** Southern Colorado Plateau GCM projected mean November–March total precipitation (mm), 2050. Lower left: 22-Model ensemble; Upper left: HAD; Upper right: ECHAM. See Table 1 for GCM acronyms.

models show greater agreement with each other, with prominent drying in the western two-thirds of the domain. The two models project a slight increase in May–June precipitation for the eastern part of the SCP domain, in contrast to the 22-ME projection.

For November–March mid-century projections, similarly, the two models show a slight increase in precipitation for much of the SCP, while the 22-model ensemble projects a slight decrease in the southern half of the SCP (Figure 11; Table 4).

**Table 4.** Qualitative assessment of precipitation projections for mid-century (2050) are compared to observations (1950–1999) for the Southern Colorado Plateau (SCP; see Figure 1). Each bold outlined box represents the SCP, and each quadrant of a bold outlined box represents one quadrant of the domain, corresponding to Figure 1 (clockwise from left, NW NE, SE, SW). Sign indicates the direction of projection; boldness indicates the magnitude of the projection. **+** large increase; + increase; – decrease; **—** large decrease.

| Model | Winter PPT (Nov-Mar) | | Spring PPT (May-Jun) | | Summer PPT (Jul-Sep) | |
|---|---|---|---|---|---|---|
| 22-Model Ensemble | + | + | **—** | – | + | + |
| | – | – | **—** | – | + | + |
| UKMO-HADGEM1 | + | + | – | – | **+** | **+** |
| | + | – | – | – | **+** | **+** |
| MPI-ECHAM5 | + | + | – | – | **—** | – |
| | – | – | **—** | – | **—** | – |
| CSIRO-MK3 | + | + | – | – | – | – |
| | + | + | **—** | – | – | – |
| CNRM-CM3 | – | – | **—** | — | + | – |
| | – | – | **—** | — | + | – |
| NCAR-CCSM3 | – | – | **—** | – | **+** | + |
| | – | – | – | – | **+** | + |

## DISCUSSION

### Model Selection and Vegetation Modeling

The fact that two GCMs included in this study captured the global extremes of temperature sensitivity as tested by Timbal et al. (2008) suggests that our model-selection process succeeded in bracketing a range of temperature increases, which is important for modeling potential changes in vegetation distribution. In all seasonal precipitation projections, the ensemble projection falls about midway between the projections by the selected models, suggesting the five selected models are showing variability similar to the full set of 22 models. (N.B.: Results from a separate analysis, using the ensemble mean of the five highest ranking models [Table 1], do not differ dramatically from the major findings of the analysis presented herein). As with temperature sensitivity, the selected models span the full range of precipitation projections, which suits the goal of the selection process in capturing the range of possibilities for bracketing potential vegetation responses.

The approach used here should bracket the inputs for future vegetation change in much

the same way as would a sensitivity analysis, although the results contain no information on the likelihood of a particular outcome. For instance, a sensitivity analysis might involve using all 22 models and Monte Carlo simulation or similar resampling approach to develop a suite of statistically robust projections of temperature and precipitation values for every month this century for input into a study of potential vegetation change (*sensu* Frey and Patil 2002). In the absence of that computationally extensive effort, multiple AOGCMs in ensembles can be used to provide more robust estimates of the mean climate state of the future, while projections from individual models can be used to provide estimates of annual variability and to consider the potential impacts if outliers become reality. Exploring a range of possibilities, using both climate and vegetation models, could help resource managers who are interested in developing adaptation plans that are robust to many possible futures (CCSP 2009, Dessai 2009), including those extreme possibilities that lie at the tails of probability distributions—which may have a small probability of occurrence, but a high probability of causing massive impact if realized.

## Implications for the Southern Colorado Plateau

Based on the results described above, the Southern Colorado Plateau annual temperatures are projected to increase by 1.5° to 3.6°C by mid-century (22-ME = 2.9°C), and by 2.53° to 5.4°C by the end of the century (22-ME = 4.0°C), with annual temperatures exceeding the 1950–1999 range of variability by the 2030s. Annual precipitation changes are less clear. A conservative estimate, using the 22-model ensemble average, indicates that SCP annual precipitation may decrease by 6% by the end of the century. The clearest indication is that SCP May–June arid foresummer precipitation is likely to decline, by 11 to 45% (conservatively, 25%). Though a small fraction of annual precipitation falls during the arid foresummer, temperatures during this time of year may be implicated in massive forest mortality (Breshears et al. 2005, Weiss et al. 2009 [in press]). The majority of twenty-first century precipitation variations do not consistently exceed the range of historic variability.

The aforementioned results are consistent with IPCC AR4 projections, and with studies that have examined projections for northern California (Dettinger 2005) and the Upper Colorado River Basin (Christensen and Lettenmaier 2007). The hydroclimatic implications of increasing temperatures coupled with precipitation variability dominated by interannual and decadal change, but lacking trend, are well known. These include decreasing snowpack (Mote et al. 2005, Rauscher et al. 2008), early snowmelt (Stewart et al. 2004, 2005, 2009), an increased fraction of liquid winter precipitation (Knowles et al. 2006), decreased runoff (Milly et al. 2005, Ellis et al. 2008), and increased evapotranspiration (Hamlet et al. 2007).

The downscaling approach used in this study does not preserve within-month variability; consequently, ephemeral daily time-scale events such as flood-producing intense rains, frosts, extreme daily temperatures, and wilt-inducing hot, dry episodes are not captured. Studies by Diffenbaugh et al. (2005), using regional climate models, and Meehl et al. (2004) show that projected increases in mean temperature across North America are associated with the aforementioned phenomena—all of which have strong effects on vegetation. In particular, temperature-limited growth processes and the combination of increased temperatures and soil moisture deficits can affect widespread tree mortality and treeline conifer species distribution (e.g., Adams et al. 2009, van Mantgem et al. 2009, Schrag et al. 2008). Moreover, Weiss et al. (2009

[in press]) demonstrate that increased late spring temperatures and drying, consistent facets of the projections used in this study, increase evapotranspirational demand and vegetation moisture stress.

The approach used in this study did preserve annual and multidecadal climate variability, which can be important to vegetation changes. The use of individual model projections allows a more robust simulation of time-series annual and multidecadal climate fluctuations for vegetation modeling than the ensemble mean, though the statistical characteristics of multi-model ensembles are more robust for examining trends and mean values for specified time periods (Pierce et al. 2009). Annual and seasonal variability can influence many ecological processes that can affect species distribution, including seedling germination and survival, herbivore pressure, pollinator phenology, and wildfire frequency and extent. For example, dry wildfire seasons that follow relatively wet years can be associated with more area-burned than dry seasons following dry years in some cases (Swetnam and Betancourt 1998).

## CONCLUSIONS

In this study, we statistically downscaled selected IPCC AR4 GCMs for the western United States. Our statistical downscaling method rapidly, and at little cost, provided simulations of future climate at a spatial scale acceptable for input to process-based landscape-scale vegetation models. GCMs were selected for their simulation of western U.S. precipitation, and for characteristics that would produce a range of future climatic conditions to drive vegetation change simulation models for the Southern Colorado Plateau. Our evaluation of selected models, based on their simulation of the seasonal cycle of precipitation and spatial correlation between GCMs and observed precipitation, revealed that all overestimate annual SCP precipitation, and that few match the observed SCP seasonal cycle of precipitation. Models better estimated the seasonal cycle of SCP temperatures, but several models exhibited biases toward warmer than observed summer temperatures and cooler than observed winter temperatures. The HAD model displayed the closest match with historic precipitation observations, but some of the projections from HAD, notably summer precipitation, are well beyond the edge of the envelope of projections of other models.

Projections of future temperature and precipitation, based on individual models and a 22-model ensemble mean, show excellent agreement with regard to projecting temperature increases for the SCP; however, differences in magnitude between GCMs spanned more than 3°C in each season, and for annual temperature. For future precipitation, the most important results are (1) the models show only slight downward trends in annual and winter precipitation and no trend in fall and summer, and (2) the selected models show a strong downward trend in May–June precipitation. In combination with increasing temperatures, lack of moisture during this time of year could increase the likelihood of massive forest mortality events, such as the die-off of Colorado Plateau conifers in the early part of the twenty-first century.

Our analysis demonstrated that the models selected for vegetation analysis produce substantially greater variability than ensembles (an obvious result) and, in this case, a rich array of variability and potential future climates. The approach used here lends itself to a relatively inexpensive version of a sensitivity analysis, in that ecologists can compare the effects on vegetation given the range of projections available. Recent research shows that using comprehensive sets of metrics to choose a set of "best models" does not necessarily result in better projections, but rather that including more models increases the likelihood of producing robust projections (Pierce et al. 2009)—when projections rely on estimates of mean

quantities.

One prospect for future research is to use regional climate model simulations to downscale GCM projections and retain fine-scale dynamical processes (e.g., Diffenbaugh et al. 2005). In the meantime, the approach used here, bracketing the ensemble GCMs results with plausible, but different, individual projections is one that can be applied to robust decision-making approaches advocated by some decision scientists (e.g., CCSP 2009). The use of statistically downscaled GCM projections can provide a starting point for considering the range of vegetation conditions resource managers might face in the near future and by the end of the century.

## ACKNOWLEDGMENTS

This work was funded by Department of Energy National Institute for Climate Change Research, project MPC35TV-02, "Regional Dynamic Vegetation Model for the Colorado Plateau: a Species-Specific Approach." The authors acknowledge Dr. Andrew Ellis, Arizona State University, for providing estimated potential evapotranspiration data for the Colorado Plateau region. The authors also acknowledge the communications and design staff of the University of Arizona Institute of the Environment for assistance with graphics.

## REFERENCES

Adams, H. D., M. Guardiola-Claramonte, G. A. Barron-Gafford, J. Camilo Villegas, D. D. Breshears, C. B. Zou, P. A. Troch, and T. E. Huxman. 2009. Temperature sensitivity of drought-induced tree mortality portends increased regional die-off under global-change-type drought. Proceedings of the National Academy of Sciences 106(17):7063–66. doi: 10.1073/pnas.0901438106

Bachelet, D., R. P. Neilson, T. Hickler, R. J. Drapek, J. M. Lenihan, M. T. Sykes, B. Smith, S. Sitch, K. Thonicke. 2003. Simulating past and future dynamics of natural ecosystems in the United States. Global Biogeochemical Cycles 17(2):14-1–14-21.

Brekke, L. D., Dettinger, M. D., Maurer, E. P., and Anderson, M. 2008. Significance of model credibility in estimating climate projection distributions for regional hydroclimatological risk assessments. Climate Change 89, 371–94. doi: 10.1007/s10584-007-9388-3.

Breshears, D. D., N. S. Cobb, P. M. Rich, K. P. Price, C. D. Allen, R. G. Balice, W. H. Romme, J. H. Kastens, M. L. Floyd, J. Belnap, J. J. Anderson, O. B. Myers, and C. W. Meyer. 2005. Regional vegetation die-off in response to global-change-style drought. Proceedings of the National Academy of Sciences 102(42):15144–48.

Burkett, V. R., D. A. Wilcox, R. Stottlemyer, W. Barrow, D. Fagre, J. Baron, J. Price, J. L. Nielsen, C. D. Allen, D. L. Peterson, G. Ruggerone, and T. Doyle. 2005. Nonlinear dynamics in ecosystem response to climatic change: Case studies and policy implications. Ecological Complexity 2:357–94.

CCSP. 2009. Best Practice Approaches for Characterizing, Communicating, and Incorporating Scientific Uncertainty in Decisionmaking, edited by M. Granger Morgan, Hadi Dowlatabadi, Max Henrion, David Keith, Robert Lempert, Sandra McBride, Mitchell Small, and Thomas Wilbanks. A Report by the Climate Change Science Program and the Subcommittee on Global Change Research. National Oceanic and Atmospheric Administration, Washington, D.C.

CCSP. 2008. Climate Models: An Assessment of Strengths and Limitations. A Report by the U.S. Climate Change Science Program and the Subcommittee on Global Change Research, authored by D. C. Bader, C. Covey, W. J. Gutowski, I. M. Held, K. E. Kunkel, R. L. Miller, R. T. Tokmakian and M. H. Zhang. Department of Energy, Office of Biological and Environmental Research, Washington, D.C.

Christensen, J. H., B. Hewitson, A. Busuioc, A. Chen, X. Gao, I. Held, R. Jones, R. K. Kolli, W.-T. Kwon, R. Laprise, V. Magaña Rueda, L. Mearns, C. G. Menéndez, J. Räisänen, A. Rinke, A. Sarr, and P. Whetton. 2007. Regional Climate Projections. In Climate Change 2007: The Physical Science Basis. Contribution of Working Group I to the Fourth Assessment Report of the Intergovernmental Panel on Climate Change, edited by S. Solomon, D. Qin, M. Manning, Z. Chen, M. Marquis, K. B. Averyt, M. Tignor, and H. L. Miller. Cambridge University Press, Cambridge, United Kingdom, and New York, New York.

Christensen, N., and D. P. Lettenmaier. 2007. A multimodel ensemble approach to assessment of climate change impacts on the hydrology and water resources of the Colorado River basin. Hydrology and Earth System Sciences Discussions 11(1417–34).

Coquard, J., P. B. Duffy, K. E. Taylor, and J. P. Iorio. 2004. Present and future climate in the western USA as simulated by 15 global climate models. Climate Dynamics 23:455–72.

Covey, C., K. M. AchutaRao, U. Cubasch, P. Jones, S. J. Lambert, M. E. Mann, T. J. Phillips, and K. E. Taylor. 2003. An overview of results from the Coupled Model Intercomparison Project. Global and Planetary Change 37:103–33.

Daly, C., R. P. Neilson, and D. L. Phillips. 1994. A statistical-topographic model for mapping climatological precipitation over mountainous terrain. Journal of Applied Meteorology 33:140–58.

Daly, C., G. H. Taylor, W. P. Gibson, T. W. Parzybok, G. L. Johnson, P. Pasteris. 2001. High-quality spatial climate data sets for the United States and beyond. Transactions of the American Society of Agricultural Engineers 43:1957–62.

Daly, C., W. P. Gibson, G. H. Taylor, G. L. Johnson, P. Pasteris. 2002. A knowledge-based approach to the statistical mapping of climate. Climate Research 22:99–113.

Dessai, S., M. Hulme, R. Lempert and R. Pielke, Jr., 2009. Do We Need Better Predictions to Adapt to a Changing Climate? EOS: Transactions of the American Geophysical Union 90(13):111–12.

Dettinger, M. D., 2005. From climate change spaghetti to climate change distributions for 21st century California. San Francisco Estuary Watershed Science 3(1):1–14.

Diffenbaugh, N. S., J. S. Pal, R.J. Trapp, and F. Giorgi. 2005. Fine-scale processes regulate the response of extreme events to global climate change. Proceedings of the National Academy of Sciences 102(44):15774–78.

Duffy, P. B., B. Govindasamy, J. P. Iorio, J. Milovich, K. R. Sperber, K. E. Taylor, M. F. Wehner, S. L. Thompson. 2003. High-resolution simulations of global climate, part 1: Present climate. Climate Dynamics 21:371–90.

Eischeid J. K., Pasteris P. A., Diaz H. F., Plantico M. S., Lott N. J. 2000. Creating a serially complete, national daily time series of temperature and precipitation for the western United States. Journal of Applied Meteorology 39:1580–91.

Ellis, A. W., T. W. Hawkins, R. C. Balling, and P. Gober. 2008. Estimating future runoff levels for a semiarid fluvial system in central Arizona. Climate Research 35:227–39.

Frey, H. C., and S. R. Patil. 2002. Identification and review of sensitivity analysis methods. Risk Analysis 22(3):553–78.

Govindasamy, B., P. B. Duffy, and J. Coquard. 2003. High-resolution simulations of global climate, part 2: Effects of increased greenhouse gases. Climate Dynamics 21:391–404.

Hamlet, A. F., P. W. Mote, M. P. Clark, and D. P. Lettenmaier. 2007. Twentieth-century trends in runoff, evapotranspiration, and soil moisture in the western United States. Journal of Climate 20:1468–86.

Hamon W. R. 1961. Estimating potential evapotranspiration. Proceedings of the American Society of Civil Engineering 871:107–20.

Higgins, R. W., Y. Chen, and A. V. Douglas, 1999. Interannual variability of the North American warm season precipitation regime. Journal of Climate 12:653–80.

Hoerling, M., J. Eischeid, X. Quan, T. Xu. 2007. Explaining the record U.S. warmth of 2006. Geophysical Research Letters, 34, L17704. doi:10.1029/2007GL030643.

IPCC. 2007. Climate Change 2007: The Physical Science Basis. Contribution of Working Group I to the Fourth Assessment Report of the Intergovernmental Panel on Climate Change, edited by S. Solomon, D. Qin, M. Manning, Z. Chen, M. Marquis, K. B. Averyt, M. Tignor and H. L. Miller. Cambridge University Press, Cambridge, United Kingdom. and New York, New York.

Knowles, N., M. D. Dettinger, and D. R. Cayan. 2006. Trends in snowfall versus rainfall in the western United States. *Journal of Climate* 19(18):4545–59.

Kripalani, R. H., J. H. Oh, H. S. Chaudhari. 2007. Response of the East Asian summer monsoon to doubled atmospheric $CO_2$: Coupled climate model simulations and projections under IPCC AR4. Theoretical and Applied Climatology 87:1–28.

Lin, J.-L., B. E. Mapes, K. M. Weickmann, G. N. Kiladis, S. D. Schubert, M. J. Suarez, J. T. Bacmeister, and M.-I. Lee. 2008. North American monsoon and convectively coupled equatorial waves simulated by IPCC AR4 coupled GCMs. Journal of Climate 21(12): 2919–37. doi:10.1175/2007 JCLI1815.1.

Logan, J. A., J. Régnière, and J. A. Powell. 2003. Assessing the impacts of global climate change on forest pests. Frontiers in Ecology and the Environment 1:130–37.

Meehl G. A., C. Covey, T. Delworth, M. Latif, B. McAvaney, J. F. B. Mitchell, R. J. Stouffer, and K. E. Taylor. 2007. THE WCRP CMIP3 multimodel dataset: A new era in climate change research, BAMS, 88:1383–94. doi 10.1175/BAMS-88-9-1383.

Meehl, G. A., C. Tebaldi, and D. Nychka, 2004. Changes in frost days in simulations of twentyfirst century climate. Climate Dynamics 23:495–511.

Milly, P. C. D., K. A. Dunne, et al. 2005. Global pattern of trends in streamflow and water availability in a changing climate. Nature 438:347–50.

Moss, R., M. Babiker, S. Brinkman, E. Calvo, T. Carter, J. Edmonds, I. Elgizouli, S. Emori, L. Erda, K. Hibbard, R. Jones, M. Kainuma, J. Kelleher, J. Francois Lamarque, M. Manning, B. Matthews, J. Meehl, L. Meyer, J. Mitchell, N. Nakicenovic, B. O'Neill, R. Pichs, K. Riahi, S. Rose, P. Runci, R. Stouffer, D. van Vuuren, J. Weyant, T. Wilbanks, J. Pascal van

Ypersele, and M. Zurek. 2008. Towards New Scenarios for Analysis of Emissions, Climate Change, Impacts, and Response Strategies. Intergovernmental Panel on Climate Change. Geneva, Switzerland.

Mote, P. W., A. F. Hamlet, M. P. Clark, and D. P. Lettenmaier. 2005. Declining mountain snowpack in western North America. Bulletin of the American Meteorological Society 86:39–49.

Nakicenovic, N., J. Alcamo, G. Davis, B. de Vries, J. Fenhann, S. Gaffin, K. Gregory, A. Grübler, T. Y. Jung, T. Kram, E. L. La Rovere, L. Michaelis, S. Mori, T. Morita, W. Pepper, H. Pitcher, L. Price, K. Raihi, A. Roehrl, H.-H. Rogner, A. Sankovski, M. Schlesinger, P. Shukla, S. Smith, R. Swart, S. Van Rooijen, N. Victor, and Z. Dadi. 2000. Special Report on Emissions Scenarios: A Special Report of Working Group III of the Intergovernmental Panel on Climate Change. Cambridge University Press, Cambridge, United Kingdom. Available online at: *http://www.grida.no/climate/ipcc/emission/index.htm.*

Pierce, D. W., T. P. Barnett, B. D. Santer, and P. J. Gleckler. 2009. Selecting global climate models for regional climate change studies. Proceedings of the National Academy of Sciences 106(21):8441–46.

Rauscher, S. A., J. S. Pal, N. S. Diffenbaugh, and M. M. Benedetti. 2008. Future changes in snowmelt-driven runoff timing over the western U.S. Geophysical Research Letters, 35, L16703. doi:10.1029/2008GL034424.

Reichler, T., and J. Kim. 2008. How well do coupled models simulate today's climate? Bulletin of the American Meteorological Society 89:303–11.

Salathé, E. P. 2005. Downscaling simulations of future global climate with application to hydrologic modelling. International Journal of Climatology 25:419–36.

Savage, M., P. M. Brown, and J. Feddema. 1996. The role of climate in a pine forest regeneration pulse in the southwestern United States. Ecoscience 3:310–18.

Schrag, A. M., A. G. Bunn, and L. J. Graumlich. 2008. Influence of bioclimatic variables on tree-line conifer distribution in the Greater Yellowstone Ecosystem: Implications for species of conservation concern. Journal of Biogeography 35(4):698–710. doi: 10.1111/j.1365-2699.2007.01815.x

Seager, R., M . Ting, I . Held, Y . Kushnir, J . Lu, and G. Vecchi. 2007. Model projections of an imminent transition to a more arid climate in southwestern North America. Science 316(5828):1181–84.

Stephenson, N., D. Peterson, D. Fagre, C. Allen, D. McKenzie, and J. Baron. 2006. Response of western mountain ecosystems to climatic variability and change: The Western Mountain Initiative. Park Science. 34(1):24–29.

Stewart, I. T., D. R. Cayan, et al. 2004. Changes in snowmelt runoff timing in western North American under a 'business as usual' climate change scenario. Climatic Change 62:217–32.

Stewart, I. T., D. R. Cayan, et al. 2005. Changes toward earlier streamflow timing across western North America. Journal of Climate 18:1136–55.

Stewart, I. T. 2009. Changes in snowpack and snowmelt runoff for key mountain regions. Hydrological Processes 23(1):78–94. doi: 10.1002/hyp.7128

Swetnam, T.W., and J. L. Betancourt. 1998. Mesoscale disturbance and ecological response to decadal climatic variability in the American Southwest. Journal of Climate 11:3128–47.

Timbal, B., P. Hope, and S. Charles. 2008. Evaluating the consistency between statistically downscaled and global dynamical model climate change projections. Journal of Climate 21:6052–59.

USDA Forest Service Southwest Region. 2008. Locations of bark beetle activity: Arizona and New Mexico. Aerial survey results posted at *http://www.fs.fed.us/r3/resources/health/beetle/index.shtml.* Accessed on 9/21/2009.

van Mantgem P. J., N. L. Stephenson, J. C. Byrne, L. D. Daniels, J. F. Franklin, P. Z. Fulé, M. E. Harmon, A. J. Larson, J. M. Smith, A. H. Taylor, T. T. Veblen. 2009. Widespread increase of tree mortality rates in the western United States. Science 323:521–24. doi: 10.1126/science.1165000

Weiss, J. L., C. L. Castro, and J. T. Overpeck. In press. Distinguishing pronounced droughts in the southwestern U.S.A.: Seasonality and effects of warmer temperatures. Journal of Climate. Revised version sent 18 March 2009.

Widmann, M., C. S. Bretherton, and E. P. Salathé. 2003. Statistical precipitation downscaling over the northwestern United States using numerically simulated precipitation as a predictor. Journal of Climate 16:799–816.